Real-time magnetic resonance imaging–guided radiofrequency atrial ablation and visualization of lesion formation at 3 Tesla

Gaston R. Vergara, MD,* Sathya Vijayakumar, MS,* Eugene G. Kholmovski, PhD,* Joshua J.E. Blauer, MS,* Mike A. Guttman, MS,† Christopher Gloschat, BS,* Gene Payne, MS,* Kamal Vij, PhD,† Nazem W. Akoum, MD,* Marcos Daccarett, MD,* Christopher J. McGann, MD,* Rob S. MacLeod, PhD,* Nassir F. Marrouche, MD, FHRS*

*From the *Comprehensive Arrhythmia Research and Management (CARMA) Center, School of Medicine, University of Utah, Salt Lake City, Utah, and †SurgiVision Inc., Irvine, California.*

BACKGROUND Magnetic resonance imaging (MRI) allows visualization of location and extent of radiofrequency (RF) ablation lesion, myocardial scar formation, and real-time (RT) assessment of lesion formation. In this study, we report a novel 3-Tesla RT -RI based porcine RF ablation model and visualization of lesion formation in the atrium during RF energy delivery.

OBJECTIVE The purpose of this study was to develop a 3-Tesla RT MRI-based catheter ablation and lesion visualization system.

METHODS RF energy was delivered to six pigs under RT MRI guidance. A novel MRI-compatible mapping and ablation catheter was used. Under RT MRI, this catheter was safely guided and positioned within either the left or right atrium. Unipolar and bipolar electrograms were recorded. The catheter tip–tissue interface was visualized with a T1-weighted gradient echo sequence. RF energy was then delivered in a power-controlled fashion. Myocardial changes and lesion formation were visualized with a T2-weighted (T2W) half Fourier acquisition with single-shot turbo spin echo (HASTE) sequence during ablation.

RESULTS RT visualization of lesion formation was achieved in 30% of the ablations performed. In the other cases, either the lesion was formed outside the imaged region (25%) or the lesion was not created (45%) presumably due to poor tissue–catheter tip contact. The presence of lesions was confirmed by late gadolinium enhancement MRI and macroscopic tissue examination.

CONCLUSION MRI-compatible catheters can be navigated and RF energy safely delivered under 3-Tesla RT MRI guidance. Recording electrograms during RT imaging also is feasible. RT visualization of lesion as it forms during RF energy delivery is possible and was demonstrated using T2W HASTE imaging.

KEYWORDS Atrial fibrillation; Catheter ablation; Lesion visualization; Radiofrequency energy; Real-time magnetic resonance imaging

ABBREVIATIONS **3D** = three dimensional; **EGM** = electrogram; **EP** = electrophysiology; **FLASH** = fast low angle shot; **GRE** = gradient-recalled echo; **HASTE** = half Fourier acquisition with single-shot turbo spin echo; **LGE** = late gadolinium enhancement; **MRI** = magnetic resonance imaging; **RF** = radiofrequency; **RT** = real time; **T1W** = T1-weighted; **T2W** = T2-weighted; **TE** = echo time; **TR** = repetition time

(Heart Rhythm 2011;8:295–303)

Introduction

Radiofrequency (RF) ablation[1] has evolved from a primitive procedure to the mainstay of arrhythmia management it is today.[2] As progress was made in the understanding of the mechanisms underlying arrhythmias, the limitations of fluoroscopy and conventional mapping techniques became apparent. Electroanatomic mapping allows for three-dimensional (3D) cardiac chamber reconstruction, spatial catheter localization, tissue characterization based on local electrograms (EGMs) and electrophysiologic tissue properties, and assessment of adequate RF energy delivery. Reduction in local tissue EGM voltage remains a widely used, albeit indirect, method for assessing adequate lesion formation. Electroanatomic mapping has become the cornerstone of modern, complex cardiac ablations.

A more effective endpoint for RF ablation would be direct, real-time (RT) visualization of myocardial destruction to assess lesion formation during ablation. Magnetic resonance imaging (MRI) allows for the assessment of location and extent of RF ablation lesion and of scar formation in the myocardium.[3] However, assessment of lesion formation during RF energy delivery has remained elusive. Several groups have reported MRI tracking of catheters

S. Vijayakumar, Dr. Kholmovski, G. Payne, and Dr. Marrouche are partially supported by grant from SurgiVision Inc. Dr. Vij and M. Guttman are employees of SurgiVision Inc. **Address reprint requests and correspondence:** Dr. Nassir F. Marrouche, CARMA Center, Division of Cardiology, University of Utah Health Sciences Center, Suite 4A100 SOM, 30 North 1900 East, Salt Lake City, Utah 84132. E-mail address: massir.marrouche@hsc.utah.edu. (Received August 30, 2010; accepted October 22, 2010.)

  doi:10.1016/j.hrthm.2010.10.032

within the cardiac chambers with successful delivery of RF energy and postprocedure visualization of lesion formation in 1.5-Tesla scanners.[4–7] This is feasible using MRI; however, to the best of our knowledge, the ability to combine RT MRI tracking of electrophysiology (EP) catheters and recording of EGMs, with actual tissue and lesion formation visualization during RF ablation, has not been described yet. A system integrating these would prove valuable because it would allow visualization of a "hard" endpoint to ablation: direct, RT visualization of myocardial scar formation and its correlation with changes in tissue electrophysiologic properties.

In this study, we report a novel 3-Tesla RT MRI-guided catheter tracking system combined with a unique RT MRI sequence and a new T2-weighted (T2W) sequence, which have allowed us to successfully and safely position an EP catheter within the atria, record intracardiac EGMs, and ablate with simultaneously RT visualization of RF myocardial lesion as it is being formed.

Methods

Catheter description and energy delivery

A 110-cm 7F, 3-mm-tip, steerable, MRI-compatible ablation catheter (SurgiVision Inc., Irvine, CA, USA) was designed to deliver RF energy under 3-Tesla RT MRI. The catheter offered impedance monitoring and unipolar and bipolar EGM recording, and was able to deliver up to 40 W of energy in a power-controlled mode. It had four tracking microcoils. Figure 1A depicts a prototype EP-MRI catheter with a close-up view showing the catheter tip and the tracking coils in a deflected catheter.

Intracardiac EGM signal recording was acquired directly from the catheter, passed through a custom-built amplifier/filter. A filter with a passband between 30 and 500 Hz was used. The signal was then displayed and stored electronically. Surface ECG tracings were directly obtained from the Veris-MR monitor (Medrad Inc., Warrendale, PA, USA) and displayed over the intracardiac recordings, allowing timing of the EGMs.

Electrical isolation between the MRI scanner and catheter was achieved by using custom low-pass filters. The layout in which components inside the MR suite are connected to the components outside through a waveguide built into the RF shield that encloses the entire MRI suite is shown in Figure 1B. The catheter was connected to a standard ablation unit (Stockert-70 RF-generator, Biosense Webster, Diamond Bar, CA, USA) with custom-built MR-compatible interface circuits.

Electrophysiology MRI interventional suite

Imaging and ablations were performed in an EP-MRI suite equipped with a 3-Tesla Siemens Verio scanner (Siemens Healthcare, Erlangen, Germany), adjacent to the conventional EP suite. The animals were transferred between the EP-laboratory and the EP-MRI suite, using a system of rails (Siemens Angio-MR Miyabi, Siemens Healthcare).

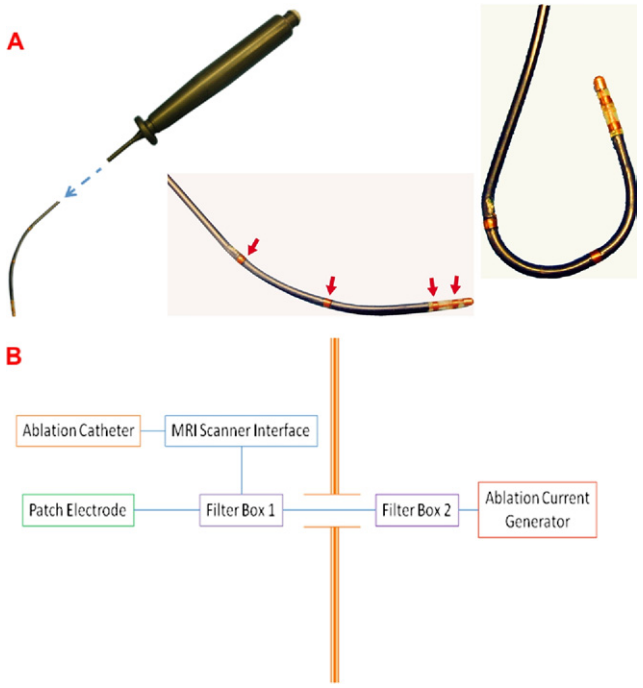

Figure 1 Prototype of the magnetic resonance imaging (MRI)-compatible ablation catheter and schematic setup of the ablation delivery system and components inside and outside the EP-MRI suite. **A:** A 7F, 110-cm, MRI-compatible radiofrequency ablation catheter. The catheter uses a plunger mechanism for deflection. *Red arrows* indicate the four tracking microcoils. **B:** Setup for ablation and radiofrequency delivery system. The ablation catheter, MRI scanner interface, MRI scanner, patch electrode, and one of the filter boxes are in the EP-MRI suite. A second filter box and a standard ablation current generator are housed outside.

Four projectors attached to the MRI host and RT MRI computers, ablation unit, and telemetry system projected their images through waveguides onto MRI-compatible projection panels inside the EP-MRI suite. These images provided the operator in the MRI suite with the same RT information that the MRI physicist/technologist received outside of the room.

Hearing protection and communication with the personnel outside was achieved with a fiberoptic communication system (Opto Acoustics Inc., Or-Yehuda, Israel).

Animal experiments

Six female pigs were used for the study. All animals were between 6 and 12 months old. Mean weight of the animals was 40.4 ± 10 kg. Animal protocols were approved by the Institutional Animal Care and Use Committee.

Anesthesia was induced and maintained with intravenous sodium pentobarbital. The animals were mechanically ventilated during the experiment. Monitoring of vital signs was performed using a Veris vital signs monitor. Intravenous access was obtained via surgical cutdown. In two of the six animals, left atrial access was obtained. Transseptal puncture was performed with an MRI-compatible sheath under intracardiac echocardiography and fluoroscopy guidance.

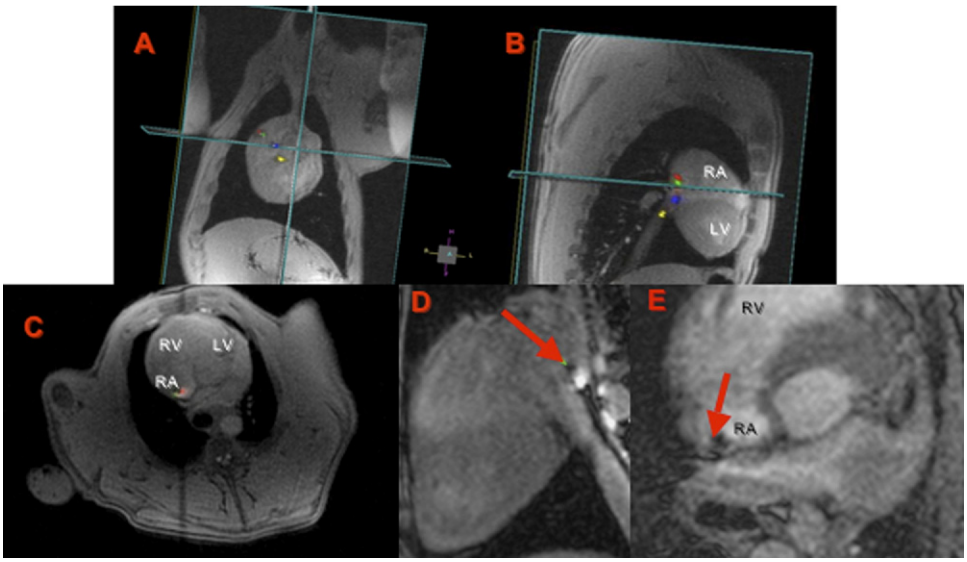

Figure 2 Assessment of catheter tip position and catheter tip–tissue interface by real-time magnetic resonance imaging (MRI) and FLASH sequences. An MRI-compatible catheter is guided under real-time MRI (**A–C**) from the inferior vena cava to the lateral wall of the right atrium (RA). This is seen in orthogonal planes (coronal, sagittal, and axial views). **D, E:** high-resolution T1W-FLASH images show the tip of the ablation catheter touching the atrial wall *(red arrow)*. LV = left ventricle; RV = right ventricle.

Following transseptal puncture, the animals were transferred to the EP-MRI suite.

Standard spine and body array coils (Siemens Healthcare) were used for imaging. The RT sequence and T2W half Fourier acquisition with single-shot turbo spin echo (HASTE) sequences were optimized for the animal's heart rate, optimal tissue–blood contrast, and fat suppression. The MRI-compatible ablation catheter was advanced into the right or left atrium under RT MRI guidance (Figures 2A–2C). Once within the atria, different locations suitable for RF lesion delivery were chosen.

MRI and lesion visualization

The catheter was visualized during navigation with an RT MRI sequence (RF spoiled gradient-recalled echo [GRE] pulse sequence with frame rate of 5.5 fps). RT images were acquired sequentially on multiple slices and rendered in 3D space at their respective locations. This allowed device-only projection views to show the parts of the catheter outside the imaging planes.[8] Typical scan parameters for RT-GRE sequence were as follows: echo time (TE) = 1.5 ms, repetition time (TR) = 3.5 ms, flip angle = 12°, slice thickness = 4 mm, resolution = 1.8 × 2.4 mm, image matrix = 192 × 108, bandwidth = 650 Hz/pixel, and parallel imaging with reduction factor (R) = 2.

Once the catheter was in position for ablation, its tip was located using a T1-weighed (T1W)-FLASH sequence in two orthogonal planes (Figures 2D and 2E). Typical scan parameters for this 3D FLASH sequence were as follows: ECG triggered, TE/TR = 1.2/2.8 ms, flip angle = 12°, slice thickness = 2.5mm, resolution = 1.25 × 1.5 mm, image matrix = 240 × 180 × 12, bandwidth = 870 Hz/pixel, and parallel imaging with R = 2. This scan was performed during breath-hold, and typical scan time was 12 to 18 seconds. This sequence allowed high-resolution visualization of the catheter tip–myocardium interface. The arrows in Figures 2D and 2E point to a dark spot corresponding to the tip of the catheter.

Images during actual RF energy delivery were acquired using an ECG-triggered, respiratory-gated T2W-HASTE sequence. The HASTE sequence parameters were as follows: TE = 79 ms, TR = one respiration cycle, three contiguous slices with thickness of 4 mm, resolution = 1.25 × 1.78 mm, fat saturation and parallel imaging with R = 2.

At the end of the ablation, 0.2 mmol/kg of MRI contrast (Multihance, Bracco Diagnostic Inc., Princeton, NJ, USA) was injected, and late gadolinium enhancement (LGE) images were acquired 20 minutes later with a respiratory-gated 3D acquisition as previously described.[9,10] The atria were then segmented from the 3D LGE images, and a maximum-intensity projection image was generated to localize and compare the ablation lesions with the results seen on the gross specimens. This last set of images was used to confirm the presence of lesions visualized during ablation with the T2W-HASTE sequence. As previously described by our group[11] and by others,[12] LGE imaging can be used to detect postablation scar in the atrial wall.

Tissue and macroscopic examination

Following the experiment, the animals were euthanized with intravenous potassium chloride. The animal chest was opened and the lungs, pericardium and heart inspected. The heart was harvested and opened for macroscopic inspection. The right atrium was opened with a linear incision connecting the superior with the inferior vena cava and the left atrium with a line transverse to the roof and lateral wall or by incision around the ventricular side of the tricuspid and mitral annulus. Lesion characteristics were observed directly on the gross specimens. Lesion measurements (largest linear dimensions) were made and correlated with the lesion size observed on T2W-HASTE imaged at different time points from start of RF energy delivery. The ex vivo and MRI based measurements were performed in blinded fashion by two experts.

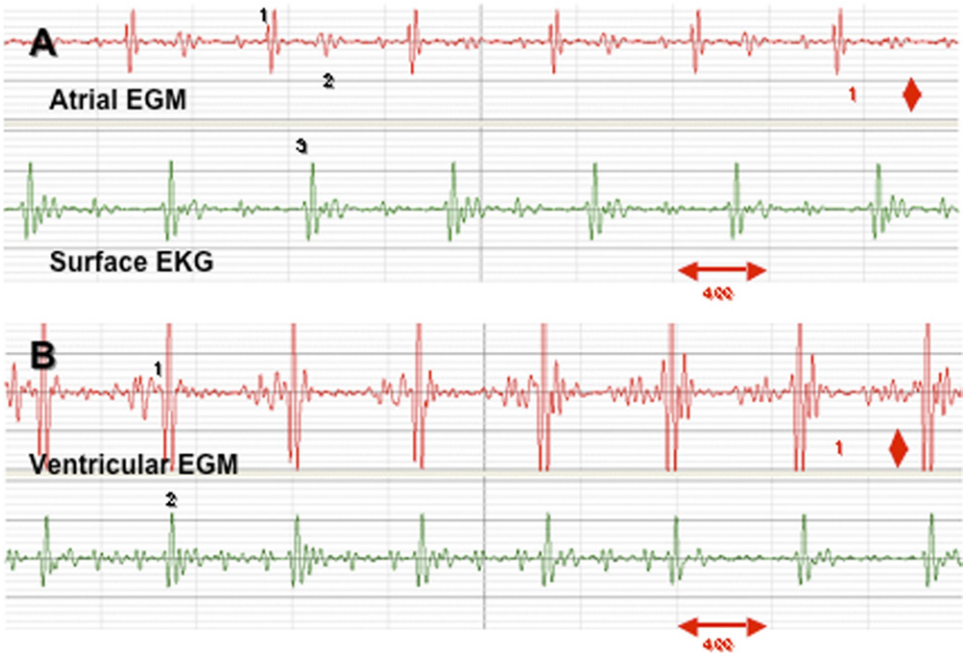

Figure 3 Bipolar atrial and ventricular intracardiac recordings obtained during real-time magnetic resonance imaging scanning. **A:** The tracing on top *(red)* represents an atrial bipolar intracardiac electrogram (1) and a far-field ventricular signal (2). The presence of the QRS (3) on surface ECG *(green)* confirms the timing and location of these recordings. **B:** The tracing on top *(red)* represents a ventricular bipolar intracardiac electrogram (1) superimposed on a surface QRS (2).

Results

Catheter testing, navigation, and recording of intracardiac EGMs

The catheter underwent heat testing at 3 Tesla and found to be less than 2° above baseline during RT MRI. The tracking elements allowed for catheter visualization during navigation. Navigation was tried at different frame rates by different operators. It was found that 5.5 fps provided a reasonable balance between good visual resolution and imaging time for all operators. Hence, our RT MRI guidance was performed using an RT GRE pulse sequence at 5.5 fps.

Intracardiac recordings

Unipolar and bipolar intracardiac EGMs were recorded during RT MRI. Figure 3 shows two typical bipolar atrial and ventricular EGMs obtained with the catheter, superimposed on a surface ECG recording.

Catheter tracking

The catheter had four tracking microcoils for guidance during RT MRI. The most distal tracking coil was 5 mm from the catheter tip. The signal from these tracking devices was color coded (red: distal; yellow: proximal; blue and green: middle) to allow the operator to clearly identify each portion of the distal end of the catheter (Figures 2A–2C).

MRI sequences and image acquisition

Resolution of the RT sequence did not allow for accurate detection of the catheter tip position. This was overcome by using high-resolution 3D T1W-FLASH scan in orthogonal planes for catheter tip–myocardium interface visualization (Figures 2D and 2E). The location of the image volume for this T1W-FLASH scan was obtained from RT MRI images. Subsequently, the position of the catheter tip detected from T1W-FLASH images was used to prescribe the T2W-HASTE slices for myocardial tissue/injury visualization during RF energy delivery (Figure 4). By performing this stepwise approach, we were able to localize specific points within the atrium and deliver RF lesions while simultaneously visualizing the tissue for immediate assessment of tissue injury and lesion formation. Figure 4 shows the localization of the catheter tip using the T1W-FLASH sequence, followed by the same location acquired using the T2W-HASTE sequence. The arrow indicates a position of catheter tip (in this case at the septal wall) within the atrium where RF energy was delivered.

Tissue edema and injury were visualized almost immediately after initiation of RF energy delivery to the atrial myocardium. LGE-MRI imaging postablation confirmed the presence of a lesion. Figure 4 shows the typical progression of lesion formation after the first few seconds of power-controlled RF energy delivery throughout 120 seconds.[13]

Animal experiments and tissue examination

Energy delivery characteristics

Twenty ablations were performed using RF application in the right and left atria under MRI guidance. Ablations in the right atria included a single ablation with 15 W for 60 seconds at 175-Ω impedance; nine with 20 W for a mean time of 67 seconds (range 25–120 seconds) and mean impedance of 117 Ω (range 99–142 Ω); and three using 25 W for a mean time of 41 seconds (range 22–60 seconds) and mean impedance of 145 Ω (range 137–160 Ω). Ablations in the left atrium included a single ablation with 15 W for 20 seconds; three using 20 W for a mean time of 60 seconds;

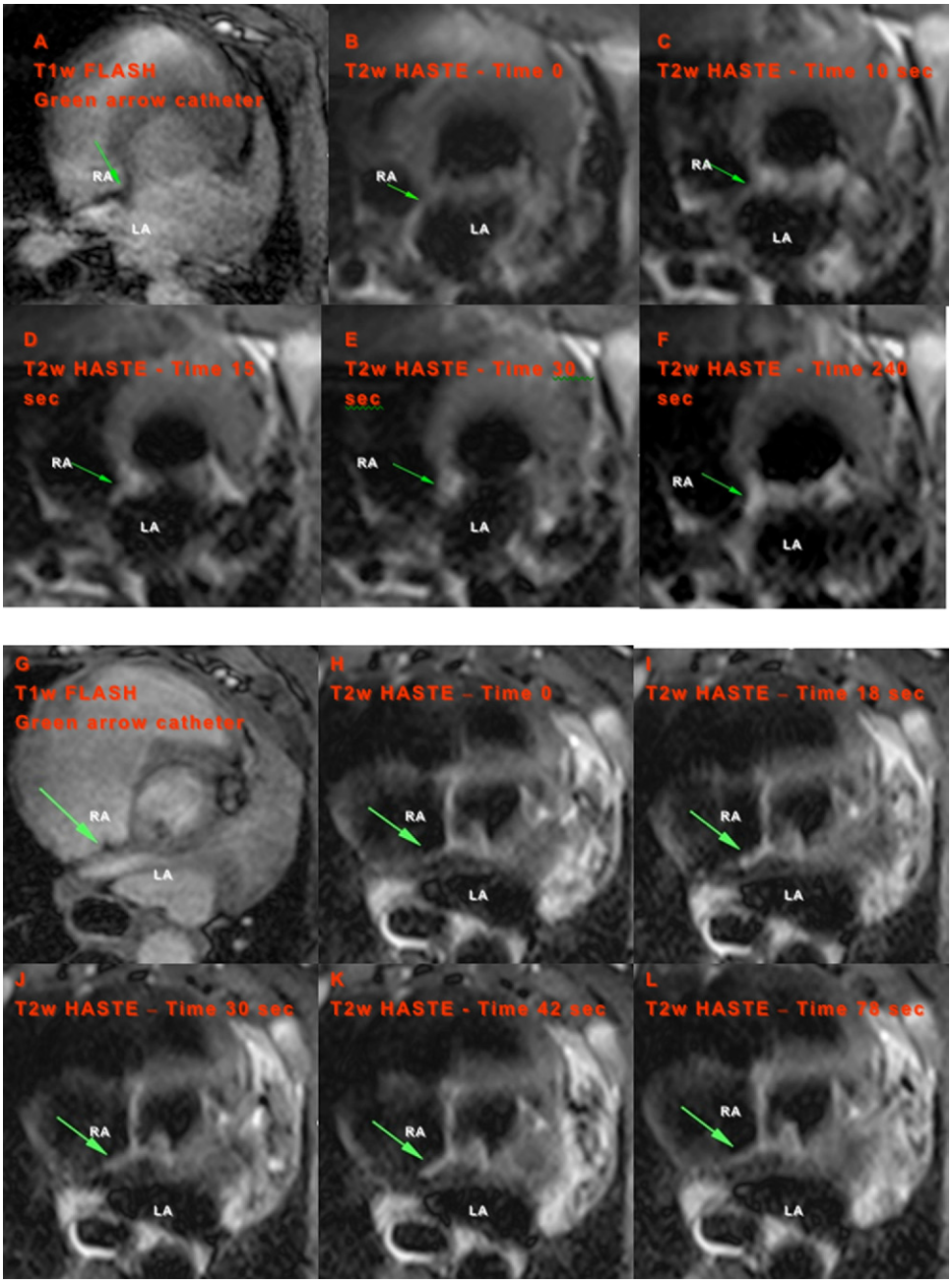

Figure 4 Catheter tip–tissue interface imaging and lesion formation visualization on the atrial septum. **A, G:** Catheter tip localization from T1W-FLASH sequence. *Green arrow* indicates catheter tip position. B–F, H–L: Temporal progression of lesion formation in the right atrium (RA) visualized by T2W-HASTE during radiofrequency energy delivery (20 W, 120 seconds; and 20 W, 90 seconds, respectively). Time after start of the ablation is shown in each image: **(B)** at the beginning of ablation and **(C–F)** 10, 15, 30, and 240 seconds after the start of the ablation, respectively; **(H)** at the beginning of ablation and **(I–L)** 18, 30, 42, and 78 seconds from the start of ablation, respectively. LA = left atrium.

and three using 25 W for a mean time of 50 seconds (range 22–60 seconds).

Lesion visualization, size, and temporal behavior

Six (30%) lesions (four in RA and two in LA) were successfully visualized during ablation. All lesions were visualized acutely during RF energy delivery as they formed and were later confirmed with LGE imaging and ex vivo examination. Nine ablations did not create any lesions, presumably due to poor catheter–tissue contact. Five lesions were not seen during ablation (four in RA and one in LA). For these five lesions, the ablation site was one to two slice planes away from the acquired HASTE imaging plane, resulting in imaging of a different area than that ablated. The lesions were visualized 90 to 120 seconds postablation when a larger volume was imaged using T2W-HASTE. Good catheter tip–tissue contact and accurate detection and imaging of catheter tip position were critical steps for successful visualization of lesion formation during ablation.

The earliest stages of lesion formation during power-controlled RF energy delivery were visualized with the use of T2W-HASTE sequence (Figures 4B–4F and 4H–4L). As early as 10 to 15 seconds after the start of ablation, tissue enhancement (associated with injury) was seen in the atrial wall. Initially, a focal T2W signal was seen at the site (Figures 4C–4E) with little to no signal in the adjacent tissue. Four minutes after RF energy delivery, repeat T2W imaging showed persistent signal intensity consistent with lesion formation at the ablation site (Figure 4F). The tem-

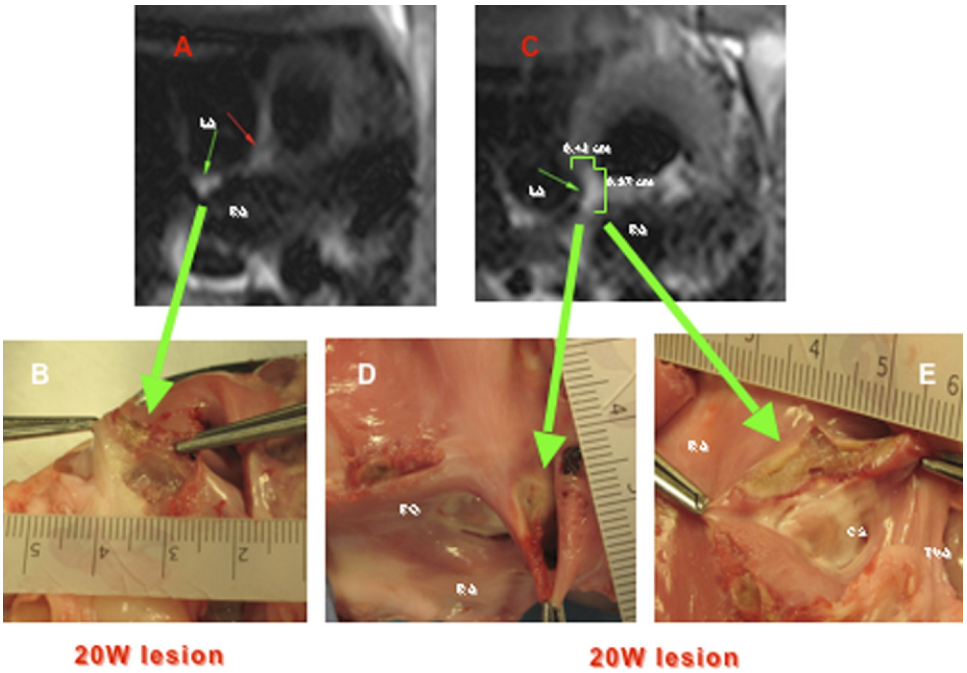

Figure 5 Correlation between real-time magnetic resonance imaging (MRI) findings during lesion formation (T2W-HASTE) and macroscopic tissue samples. **A:** T2W-HASTE image acquired 20 seconds from the start of a 20-W ablation for 90 seconds (impedance 100 Ω) shows a lesion in the posterior wall of the RA *(small green arrow).* This lesion measured approximately 5 mm in diameter by 2 mm in depth on macroscopic examination *(large green arrow* in **B**). **C:** T2W-HASTE image sequence acquired during the first 20 seconds from the start of a 20-W ablation for 120 seconds (impedance 95 Ω) shows a lesion in the cavotricuspid isthmus. This lesion measured approximately 10 mm in diameter by 4 mm in depth on macroscopic examination *(large green arrows* in **D** and **E**). CS = coronary sinus os; FO = fossa ovalis; LA = left atrium; RA = right atrium; TVA = tricuspid valve annulus.

poral changes in the tissue reflect acute edema and inflammation triggered by heat injury. LGE-MRI imaging postablation confirmed the presence of a lesion. Figure 4 (B–F and H–L) demonstrates the typical progression of lesion formation.

As expected, lesion size and depth increased with the duration of energy delivery. There was a positive correlation between total duration of energy delivery and lesion diameter and depth. This correlation is illustrated by Figure 5. Here a power-controlled 20-W lesion for 90 seconds (impedance 100 Ω) in the posterior wall of the right atrium is seen. This lesion measured approximately 5 mm in diameter by 2 mm in depth. Figure 5 also shows a 20-W power-controlled 120-second lesion on the cavotricuspid isthmus. This lesion was larger than the previous one, measuring approximately 10 mm in diameter by 4 mm in depth. This was evident on T2W-HASTE sequence imaging of the lesion and on macroscopic examination.

The transmural extent of the lesions in the left atrial appendage was clearly visualized by T2W-HASTE sequences and the extent compared well with macroscopic tissue examination and ex-vivo LGE imaging (Figure 6).

Multiple T2W-HASTE images were acquired at different time points following the start of RF energy delivery. Four of the six RT visualized lesions were used to compare measurements in MRI and ex vivo. Table 1 compares the MRI measurements made from four different RA lesions (primarily on the septal wall and lateral wall) created with similar ablation parameters (20 W, 60 seconds) at two different time points during RF energy delivery (largest linear dimension of enhancement on T2W-HASTE imaging) to similar measurements made ex vivo. The two LA lesions were not used for this correlation because on one of the animal's ex vivo examination, the incision made was such that the lesion was cut off, and in the other one animal, in the appendage, the lesion could not be measured accurately ex vivo due to fine tuberculation in the tissue. Figure 7 shows the correlation curves plotted from these measurements made about 15 to 20 seconds from the start of ablation and about 30 to 40 seconds from the start of ablation. Figure 7 shows that the earliest observed tissue changes, typically within 15 to 20 seconds of starting RF energy delivery, correlate well to the ex vivo lesion measurements. In addition, because T2W-HASTE mainly visualizes tissue edema and edema is known to spread farther out than the region of acute injury with time, images acquired later from the start of ablation are more likely to overestimate the true size of the lesion. Our results, albeit limited, indicate that for

Table 1 Lesion size from T2W HASTE and ex vivo measurements

Lesion no.	Ex vivo measurement (cm)	Time of first T2W image (seconds)	Measurement on first T2W image (cm)	Time of second T2W image (seconds)	Measurement on second T2W image (cm)
1	0.8	18	0.9	30	1.12
2	0.5	21	0.43	60	0.64
3	1.0	15	0.97	30	0.98
4	0.5	14	0.54	27	0.69

HASTE = half Fourier acquisition with single-shot turbo spin echo; T2W = T2-weighted.

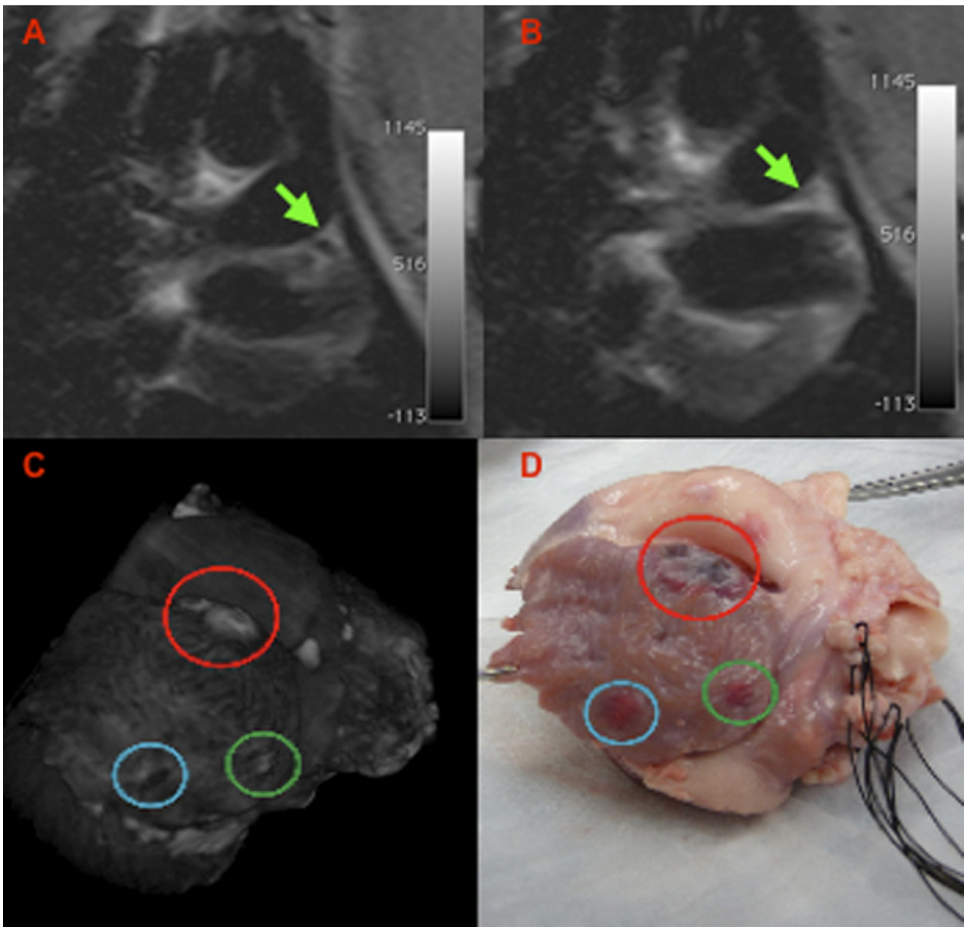

Figure 6 Correlation between T2W-HASTE images of lesion formation and three-dimensional reconstruction based on late gadolinium enhancement magnetic resonance imaging (LGE MRI) and macroscopic tissue examination in the left atrium. **A, B:** T2W-HASTE images of radiofrequency ablation in left atrial appendage. *Green arrow* points to the catheter tip **(A)** and the lesion **(B)** being formed in the left atrial appendage after power-controlled ablation (20 W, 30 seconds). **C:** Segmented, three-dimensional rendered image of an ex vivo LGE MRI scan demonstrating lesions in the left atrial appendage. *Blue circle* corresponds to the lesion depicted in **B**; red and green circles signal additional lesions in C and D. In LGE imaging a dark area is visualized, consistent with hematoma/hemorrhage within the atrial wall. **D:** Macroscopic specimen showing the lesion.

a 20-W power delivery, the T2W-HASTE images acquired about 20 seconds from the start of ablation show better correlation to actual lesion measurements ex vivo ($R = 0.92$) than those acquired about 45 seconds ($R = 0.68$) from the start of ablation.

Safety

No obvious cardiac perforation or pericardial effusion was seen during the studies. Two of the animals developed ventricular tachycardia/fibrillation with cardiac arrest, which was readily seen on the RT images and EGM traces obtained during the study. No correlation between RF energy delivery and ventricular fibrillation/ventricular could be established in these animals. The animals were quickly resuscitated by defibrillation and survived to complete the study.

Discussion

MRI-guided ablation within the atrium has recently been reported by other groups.[6,7] In one of these studies, MRI angiography of the atrium was acquired. The atrium surface was segmented, and RT catheter navigation was carried out using this 3D reconstruction. However, no images were acquired during ablation.[6] Rather, immediately postablation, lesion formation was confirmed by LGE imaging. In the other study, the catheters were navigated using RT MRI sequences.[7] However, there was no immediate tissue visualization during RF delivery and lesion formation, although there was T2W evaluation of the ablation site just before and after ablation of the cavotricuspid isthmus. Additionally, these two studies were done in 1.5-Tesla MRI.

To our knowledge, this is the first study to demonstrate RT visualization of atrial ablation lesion formation using 3-Tesla MRI. We demonstrated feasibility of navigating in the right and left atria under 3-Tesla RT MRI guidance with good catheter visualization, providing adequate temporal and spatial resolution. We were able to create lesions using RF energy delivered to the atrial myocardium while imaging the atrial tissue (with T2W-HASTE) as the lesions formed.

Imaging of lesion formation during and after ablation presented challenges due to cardiac and respiratory motion. These challenges were overcome with the use of the respiratory-gated single-shot HASTE sequence. This allowed us to visualize the effect of RF energy within the atrium. Brightness on T2W images corresponds to edema,[13] with progression to tissue destruction,[14] and scar formation, as evidenced by LGE.[12] All of the lesions visualized using T2W-HASTE were validated with postablation LGE MRI and ex vivo examination of the heart.

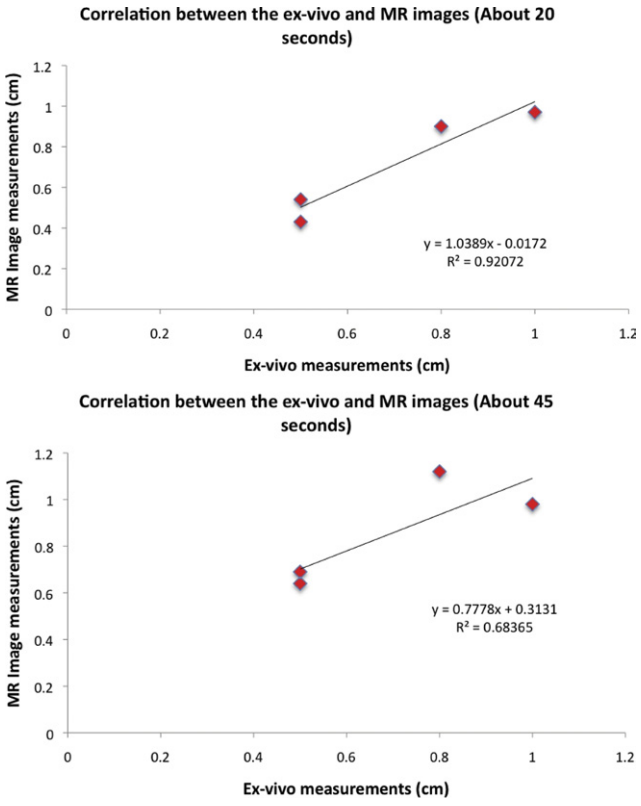

Figure 7 Correlation between enhancement size in T2W-HASTE magnetic resonance (MR) imaging *(vertical axis)* and ex vivo measurements *(horizontal axis)* of lesion for four 20-W power-controlled lesions. A correlation coefficient of 0.92 was found for the T2W-HASTE images acquired approximately 20 seconds after beginning of ablation **(top)** and a correlation coefficient of 0.68 for the T2W-HASTE images acquired approximately 45 seconds after beginning of ablation **(bottom).** The actual magnetic resonance imaging and ex vivo lesion size measurements are given in Table 1.

We were able to demonstrate a correlation between ablation time and lesion size under power-controlled RF energy delivery. This is in agreement with previously published data.[4] However, in this previous study, the time frame for imaging was much longer, and the substrate was the ventricle, which is an easier target due to the thicker myocardial wall. Also, for 20-W power delivery, the size of enhancement observed by T2W-HASTE imaging at 15 to 20 seconds from the beginning of ablation had a good correlation with the dimensions (longest diameter and depth) of the lesion on macroscopic examination. Based on our limited data, T2W-HASTE imaging at later times from the start of ablation tends to overestimate lesion size by showing the surrounding edema.

Accurate lesion visualization in the atrium still is challenging, and in our study it relied on accurate detection of catheter tip position using a high-resolution T1W-FLASH sequence and subsequently imaging this spatial location using a T2W-HASTE sequence. In some of our experiments, changes in catheter position occurred during the time interval between acquisition of T1W-FLASH images and T2W-HASTE scan. Thus, RT visualization of lesion formation was not always possible, likely because the T2W-HASTE slices did not cover the ablation location. However, even when slice alignment with the catheter tip was not feasible, after a time lapse of 90 to 240 seconds, it was possible to see lesion formation a few millimeters away from the assumed location.

Even when no specific arrhythmogenic substrate was targeted for ablation in our study, we believe that its importance lies in the possibility, for the first time, of visualizing lesion formation as it occurs in the atrium.

In summary, we developed a series of tools to navigate and guide an ablation catheter in a 3-Tesla RT MRI scanner within the right and left atria in a porcine model, record intracardiac EGMs while scanning, and deliver RF energy while simultaneously visualizing the atrial myocardium to assess for the presence of lesion formation. We were able to correlate these very early visualized lesions on T2W images with LGE MRI obtained from live and ex vivo hearts and by anatomic tissue examination (Figures 7 and 8).

This new technology presents many challenges, and there are many shortcomings to its application, such as an inability to monitor catheter tip temperature, high fidelity EGM and surface ECG recording during MRI scanning, and difficulty in RT visualization of lesion formation in many cases. Nonetheless, we believe that the work presented here is a significant advancement in the field of delivery and monitoring of RF ablation lesions, which could be potentially used as an endpoint in cardiac ablation procedures to improve outcomes.

Study limitations

Study limitations are as follows:

Catheter Steerability: The initial prototypes of MRI-compatible catheters have not been mechanically optimized to allow the operator to steer them to all parts of the atrium. Furthermore, only two standard catheter curves were available. This aspect is under continued development.

EGM Recording and Surface ECG Recording: During EGM recording, noise was present despite filtering. This prevented us from obtaining high-fidelity EGM recordings. Due to scanner interference and nonstandard surface lead placement, the elements of the surface ECG are difficult to distinguish. The QRS is visualized; however, its deflections, the P wave and T wave, are not clearly seen. We are working toward a dedicated ECG system that will provide high-fidelity recordings.

Catheter–Tissue Contact: To identify catheter tip position and to confirm catheter tip–tissue contact, a T1W-FLASH sequence was used. Occasionally this proved to be challenging, and a lesion could not be delivered and/or clearly visualized while RF energy was delivered due to lack of contact between catheter tip and myocardium or misalignment between catheter tip position and T2W-HASTE slices. This could explain why only 11 of 20 ablations resulted in lesion formation, and six of these lesions were visualized in RT.

Catheter Temperature Monitoring: The inability to monitor temperature RT was a significant limitation. Nevertheless, we showed that despite the lack of temperature mon-

itoring, an appropriate myocardial lesion could be delivered and its progression monitored in RT.

References

1. Mitsui T, Ijima H, Okamura K, Hori M. Transvenous electrocautery of the atrioventricular connection guided by the His electrogram. Jpn Circ J 1978;42: 313–318.
2. Andrikopoulos G, Tzeis S, Maniadakis N, Mavrakis HE, Vardas PE. Cost-effectiveness of atrial fibrillation catheter ablation. Europace 2009;11:147–151.
3. Dickfeld T, Kato R, Zviman M, et al. Characterization of acute and subacute radiofrequency ablation lesions with nonenhanced magnetic resonance imaging. Heart Rhythm 2007;4:208–214.
4. Nazarian S, Kolandaivelu A, Zviman MM, et al. Feasibility of real-time magnetic resonance imaging for catheter guidance in electrophysiology studies. Circulation 2008;118:223–229.
5. Kolandaivelu A, Lardo AC, Halperin HR. Cardiovascular magnetic resonance guided electrophysiology studies. J Cardiovasc Magn Reson 2009;11:21.
6. Schmidt EJ, Mallozzi RP, Thiagalingam A, et al. Electroanatomic mapping and radiofrequency ablation of porcine left atria and atrioventricular nodes using magnetic resonance catheter tracking. Circ Arrhythm Electrophysiol 2009;2: 695–704.
7. Hoffmann BA, Koops A, Rostock T, et al. Interactive real-time mapping and catheter ablation of the cavotricuspid-isthmus guided by magnetic resonance imaging in a porcine model. Eur Heart J 2010;31:450–456.
8. Gutman MA, Ozturk C, Raval AN, et al. Interventional cardiovascular procedures guided by real-time MRI: an interactive interface using multiple slices, adaptive projection modes and live 3D renderings. J Magn Reson Imaging 2007;26:1429–1435.
9. Badger TJ, Adjei-Poku YA, Burgon NS, et al. MRI in cardiac electrophysiology: the emerging role of delayed-enhancement MRI in atrial fibrillation ablation. Future Cardiol 2009;5:63–70.
10. Peters DC, Wylie JV, Hauser TH, et al. Detection of pulmonary vein and left atrial scar after catheter ablation with three-dimensional navigator-gated delayed enhancement MR imaging: initial experience. Radiology 2007;243: 690–695.
11. Badger TJ, Daccarett M, Akoum NW, et al. Evaluation of left atrial lesions after initial and repeat atrial fibrillation ablation: lessons learned from delayed-enhancement MRI in repeat ablation procedures. Circ Arrhythm Electrophysiol 2010;3:249–259.
12. Peters DC, Wylie JV, Hauser TH, et al. Recurrence of atrial fibrillation correlates with the extent of post-procedural late gadolinium enhancement: a pilot study. JACC Cardiovasc Imaging 2009;2:308–316.
13. Boxt LM, Hsu D, Katz J, et al. Estimation of myocardial water content using transverse relaxation time from dual spin-echo magnetic resonance imaging. Magn Reson Imaging 1993;11:375–383.
14. Lardo AC, McVeigh ER, Jumrussirikul P, et al. Visualization and temporal/spatial characterization of cardiac radiofrequency ablation lesions using magnetic resonance imaging. Circulation 2000;102:698–705.